Available online at www.sciencedirect.com

ScienceDirect

Physics Procedia 12 (2011) 410–418

Physics Procedia

LiM 2011

Post-Weld Residual Stress Mitigation by Scanning of a Defocused Laser Beam

Florian Tölle[a,]*, Andrey Gumenyuk[a], Moritz Oliver Gebhardt[a], Michael Rethmeier[a]

[a]*Federal Institute for Materials Research and Testing, Unter den Eichen 87, 12205 Berlin, Germany*

Abstract

High welding residual stresses can cause service life reducing consequences. Even though many processes have been developed to reduce these stresses, they are only applicable for wider welds and simple component geometries or are cost-intensive, respectively. The presented method uses a defocused beam after welding for heating the material regions on both sides of the weld. In this way, the welding stresses are decreased without contacting the surfaces using the available equipment. Different process parameters could be used depending on the component geometry and the laser power. The mechanism and the influence of the process parameters were investigated by FEM-simulation and experiments on S355J2+N steel and showed a stress reduction of about 73 %.

Keywords: residual stresses; stress reduction; high energy beam welding; post-weld heat treatment; laser scanner optics

1. Introduction

In welding, and especially in beam welding, a small material region is rapidly heated up above the melting point and cooled down back to the ambient temperature. The high temperature gradients cause high gradients in thermal expansion. Expanding material is thereby restrained by the stronger, cooler material, causing plastic deformation. During cooling, the heat-affected material shrinks and the temperature and phase depending yield strength rises and causes high tensile stresses in the weld [1]. The residual stresses in welds can reach the material specific yield strength, especially due to high energy welding processes like laser beam welding. Stresses at the local yield strength will be relaxed by plastic deformations [2, 3]. These high stresses can cause service life consequences through distortions as a result of stress relaxation or due to stress corrosion cracking [2-6].

For reducing the welding residual stresses and increasing the lifetime of welded components many processes have been developed like stress relief annealing [2, 7, 8] or the low-stress-no-distortion-technique [8-14]. But such methods are only applicable for wider welds such as TIG welds and for simple component geometries or they are cost-intensive. Beam welding processes offer the advantages of low component deformations, low heat input [4] and

* Corresponding author. Tel.: +49-30-8104-3101; Fax: +49-30-8104-1557.
E-mail address: florian.toelle@bam.de.

doi:10.1016/j.phpro.2011.03.052

remote application, which enables joining of complex component geometries. The idea behind this research work was to develop a contactless welding residual stress reduction process, which works without any additional equipment.

The presented method uses the laser beam after welding in a defocused mode for heating the material regions in a certain distance from the weld on both sides at the workpiece top surface. In these zones, compressive stresses generated by the heating process induce plastic deformations which cause tensile stresses while cooling. Through these tensile stress zones the weld is unloaded and the resulting residual stresses in the weld are decreased. The unloading mechanism and the influence of the process parameters are investigated by the finite element simulation. The simulation results are verified with experimental results.

In both the numerical and the experimental studies a 5 mm thick ferritic steel S355J2+N with specimen dimensions of 200 x 200 mm² was used. In these plates a full penetration weld was produced by a focused laser beam. Figure 1 shows the process scheme of welding and heat treatment in one work stage with the important and investigated geometric process parameters the radius r of the defocused beam, the transversal d_y and longitudinal d_x distances between the welding and the defocused beam.

Even though the very short longitudinal distances may have sense from the theoretical point of view, their practical application is restricted by particular conditions of the experiments. For the fast beam deflection to the positions of the heat treatment with the defocused laser beam a laser scanner optics was used. Due to beam defocusing by lifting the scanner optics and positioning the beam waist in specific distances above the specimen surface it is not possible to perform the welding in the same work stage as the heat treatment. This is to say that in the experiments consisting of the two work stages for welding and heat treatment, only large distances d_x and long durations, respectively, can be used. In the simulation smaller distances d_x for an in-situ process can be examined, too.

In this research study, FEM-simulation was used as a tool to investigate the process parameters in a wide range and to define useful parameter regions for practical stress reducing applications.

2. Finite element simulation for mechanism investigation and parameter study

Due to the large number of process parameters influencing the stress mitigating effect, a huge parameter matrix exists for experimental research work. The primary FEM-simulation task in this research was to perform a parameter study. This qualitative study with a simplified simulation model was expected to provide parameter regions for experimental investigations, which are most suitable for reducing longitudinal stresses in the weld and decreasing the dimensions of the process parameter matrix.

In Figure 1, the finite element mesh used in the simulations with the ANSYS-software is schematically plotted on the specimen dimension. Based on the symmetry conditions (cf. Figure 1) in the finite element model, only half of the specimen was simulated to decrease simulation time. A coarse mesh was used in the non heat treated workpiece region as shown in Figure 1 (50 mm till 100 mm in y-direction from the weld centre) with element size 6 mm x 9.7 mm because of lower temperature gradients during processing in this region. In distances between 5 mm and 50 mm elements with the dimensions of

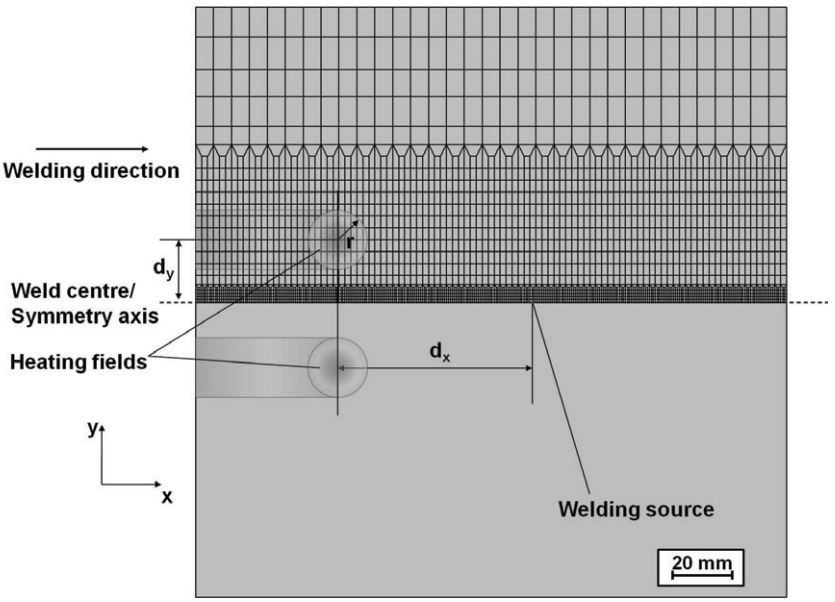

Figure 1. Process scheme for the simulation (with the used meshing model) and the experiments with the important geometric process parameters the radius r of the defocused beam, the transversal d_y and longitudinal d_x distances between the welding and the defocused beam

2 mm x 3.2 mm were used, while elements in the weld region (0 mm till 5 mm in y-direction from the weld centre) had a size of 0.7 mm x 1.1 mm. A symmetry boundary condition was applied along the weld centre line (u_y=0), while the free end at y=100 mm was ideally restrained (u_x=u_y=0).

The model was further simplified by employing an adiabatic 2D-model. In the thermal part this means, the temperature is uniformly distributed along the depth. For the structural model a plane stress approach was used, meaning that the material may freely shrink in the z-direction. The elastoplastic material model was based on the temperature dependent material properties of S355J2+N from the SYSWELD database [15]. To handle phase transformation during the welding process, a peak temperature driven approach as explained in [16] was used.

Once the models for the material, the meshing for the thermal and structural computation were developed, the models representing the heat sources had to be implemented. The welding heat source was implemented as point heat source traveled with a specified speed v_w transient in 450 steps along the axis of symmetry. Due to a non ideal Gaussian power density distribution of the defocused laser beam, the heat source representing the defocused beam for heat treatment was modeled by a cyclic area with a specified radius and a homogenously distributed power density. This heat source traveling with a specified speed v_{hf} transient in a certain transversal distance d_y to the weld centre parallel to the axis of symmetry. After the heat source had traveled in the specimen a transient cooling over 8000 seconds was performed in 47 steps. For each step of this transient analysis the thermal and structural solution was performed.

By this model the finite element simulation was used to investigate qualitatively the stress reducing mechanism of this method and the influence of the process parameters in a wide range in order to define parameter regions which are most suitable for a reduction of the welding stresses. The first simulations were carried out to determine the maximum temperature $T_{post,max}$, which has to be generated by the defocused beam in the heat treated regions, that is most suitable for the ferritic steel. In these simulations $T_{post,max}$ of around 700 °C offers the best stress reducing capability. This temperature region close to 700 °C shows a high gradient of the temperature dependent yield strength of the S355J2+N due to the α-γ-phase-transformation and the lower yield strength of the austenitic compared to the ferritic phase. As a consequence, in this temperature region the induced compressive stresses based on the heating of the material can relax through plastic deformations to give lower stress levels amounting to the local yield strength in this temperature region. During cooling to ambient temperature these plastic deformations cause tensile stresses in the heat treated zones which unload the weld in longitudinal direction due to compressing the material besides these heat treated regions, especially the material between the weld and the heat treated area.

In Figure 2, the simulation results of a welded and heat treated (with process parameters r=10 mm, d_y=27 mm, d_x=200 mm, v=5 mm/s and $T_{post,max}$=801 °C) plate are shown. In Figure 2.a the whole two-dimensional longitudinal stress profile after cooling is plotted with the positions Weld (coordinates x=100 mm and y=0 mm) and HF (coordinates x=100 mm and y=27 mm) for recording the time dependent temperature and stress profiles in Figure 2.b. With these temperature and stress profiles

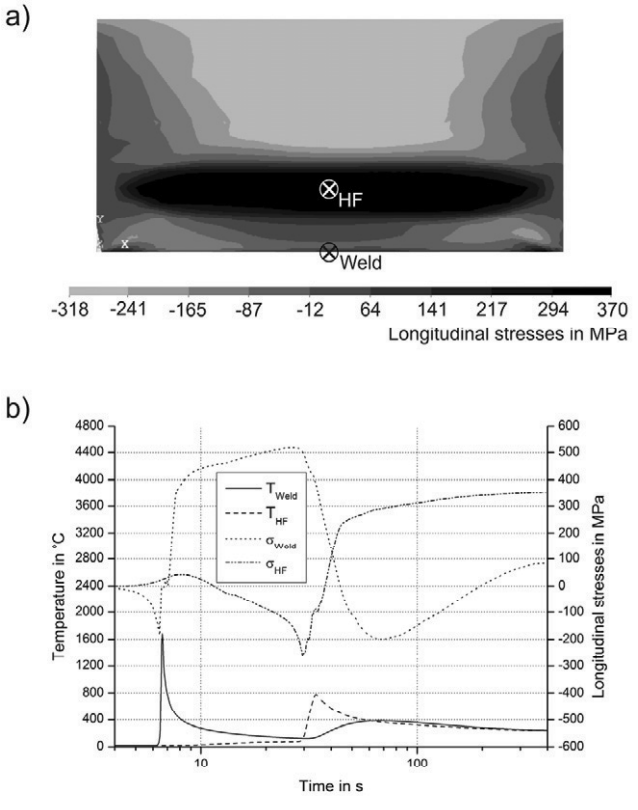

Figure 2. Simulation result of a heat treated welded plate with process parameters r=10 mm, d_y=27 mm, d_x=200 mm, v_{hf}=5 mm/s and $T_{post,max}$=801 °C: a) results of the longitudinal stresses in MPa after cooling with positions Weld and HF for temperature and stress profiles over time; b) temperature and longitudinal stress profile over time in the weld (T_{Weld}, σ_{Weld}) in x=100 mm and y=0 mm and in the centre of the heating field (T_{HF}, σ_{HF}) in x=100 mm and y=27 mm

in Figure 2.b it is possible to explain the stress mitigating process. During cooling from the melting temperature in the weld high tensile stresses were generated (cf. Figure 2.b σ_{Weld} between 7 s and 30 s). Due to heating the material region in a certain distance d_y from the weld by the defocused beam, compressive stresses were generated and relaxed in these zones while further heating to temperatures of around 700 °C based on decreasing the temperature dependent yield strength in this material region (cf. Figure 2.b σ_{HF} between 10 s and 30 s) resulting in plastic deformations. While cooling of these heated and deformed regions the compressive stresses σ_{HF} decrease and switch to tensile stresses based on the material shrinkage. These additional tensile stress zones unload the weld through compressing the material regions besides in longitudinal direction which is seen in the tensile stress decreasing in the weld represented by decreasing values of σ_{Weld} and increasing values of σ_{HF} between 30 s and 70 s. This unloading occurs as long as the temperature gradients in the heat treated regions are larger than in the weld during cooling. When the temperatures in the weld and in the heated zones are nearly the same while cooling (cf. Figure 2.b for $T_{Weld} \approx T_{HF}$ by 60 s), the unloading effect comes to a deadlock and further cooling with nearly equal temperature gradients in both regions results in an increase of the tensile longitudinal weld stresses. In consequence of the adiabatic model the simulated plate has a homogeneously distributed temperature of about 270 °C at the end of the simulations (at around 8000 s) with additional heat treatment.

For lower temperatures $T_{post,max}$ than 700 °C less stress relaxing and less plastic deformations in the heated regions are generated resulting in less stress reduction in the weld. Temperatures above 800 °C or 900 °C produce only marginal further yield strength reductions, i.e. the most suitable $T_{post,max}$ is about 700 °C for the ferritic steel S355J2+N.

Beside the temperature $T_{post,max}$, which has to be generated by the defocused beam, the geometric process parameters, i.e. the radius r of the defocused beam, the transversal d_y and longitudinal d_x distances between the welding beam and the defocused beam, exert an influence on the stress mitigating capability in the weld. The parameter d_x represents the duration between the welding and the additional heat treatment and influences the point in time till the temperature difference of T_{Weld} and T_{HF} while cooling is nearby zero and how long the unloading effect occurs. The longer the duration and the larger d_x, respectively, the stronger is the unloading effect, because of a larger temperature difference between $T_{post,max}$ and the weld temperature during cooling after the post weld heat treatment which results in a longer duration till the regions shrink in same dimensions, since these regions cool down with nearly equal temperature gradients. If d_x is very small (nearby 0 mm) no mechanical unloading occurs, because the temperature in the weld is higher than in the additionally heat treated regions.

The other geometric process parameters, i.e. the radius r of the defocused beam and the transversal distance d_y of the defocused beam from the weld interact. In Figure 3 this interaction can be seen in the most suitable d_y for stress reduction in the weld for each radius of the defocused beam. In this Figure 3

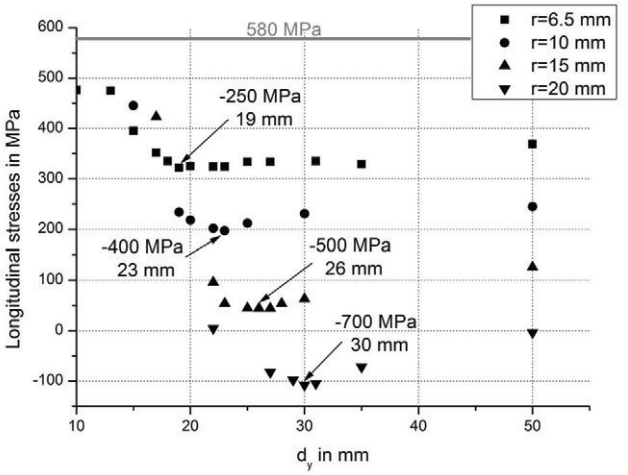

Figure 3. Correlation of the radius r and the transversal distance d_y of the defocused beam with d_x=200 mm, v_{hf}=15 mm/s and $T_{post,max} \approx 700$ °C, the longitudinal residual stresses in the weld centre are shown (stress in the weld without additional heat treatment at 580 MPa)

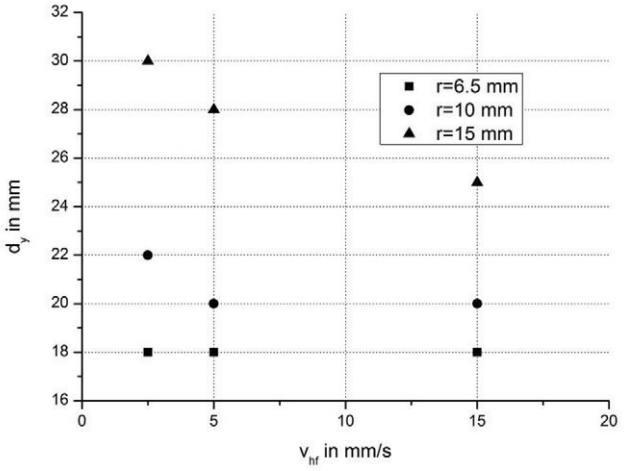

Figure 4. Correlation of travel speed v_{hf}, the radius r and the transversal distance d_y of the defocused beam with longitudinal distance d_x=200 mm and generated temperature $T_{post,max} \approx 700$ °C, showing the most suitable d_y for each radius r to be depended on v_{hf}

only the simulation results of the maximum longitudinal weld stresses depending on the transversal distance d_y of the heating field centre from the weld for the different radii r are plotted. According to these results, it may be assumed that $d_y \approx r+12$ mm offers the most suitable stress mitigating potential of this process. From the results depicted in Figure 3 larger beam radii r were expected to provide higher weld stress reducing capabilities as a consequence of larger generated tensile stress zones which unload the weld. This correlation was investigated using a high travel speed v_{hf} of 15 mm/s. For experimental applications lower travel speeds were assumed to be needed to increase the heat penetration. The simulations results depicted in Figure 4 concerning the influence of the travel speed of the defocused beam v_{hf} show only for larger radii $r \geq 15$ mm a small rise of d_y by about 5 mm as the speed was lowered from 15 mm/s to 2.5 mm/s. Lower speeds are advantageous for thick plates to generate high temperatures over the whole material thickness.

These obtained simulation results for the process parameters $T_{post,max} \approx 700$ °C, d_x (the larger the better), $d_y \approx r+12$ mm and for the minor influence of v_{hf} on d_y were verified, by performing experimental investigations in which possible stress reducing dimensions were additionally defined.

3. Experimental

In the experiments, a 5 kW fibre laser coupled with a laser scanner optics was used for welding and heat treatment in two work stages: firstly for the welding process and secondly for the heating process in which the beam was defocused and fast deflected by the special scanning optical system. To obtain different radii of the defocused beam for the heat treatment, the beam waist was positioned in certain distances above the specimen surface and the radius of the beam was measured by a laser power density meter in the workpiece level in pilot tests. The three different radii 9.5 mm, 12.0 mm and 15.5 mm including 86 % of the beam power of the defocused beam in the workpiece plane were controlled. With a thermographic camera the powers P_{hf} for heating the workpiece surface in the heating field centre to about 700 °C (cf. Figure 5 for the examples with radius r=15.5 mm) for each radius were aligned (2.3 kW, 3.5 kW and 4 kW). For the welding process, the laser beam was used in focused mode with 5 kW power and 0.3 mm radius and the welding speed was 25 mm/s. After the workpieces had cooled down to ambient temperature, the scanner optics was lifted to the adjusted distance for the specific beam radius and different powers were used for the post weld heat treatment at a travel speed of 5 mm/s on the specimen surface in the second work stage.

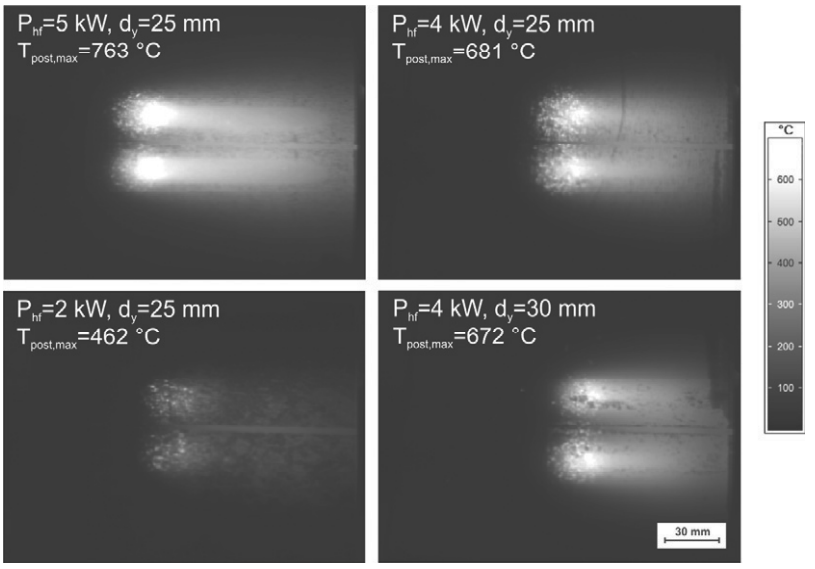

Figure 5. Measurement of the generated temperatures (in °C) in the workpiece top surface by the heat treatment with the defocused laser beam (travel speed v_{hf}=5 mm/s, radius of the heat source r=15.5 mm, longitudinal distance between welding source and heating fields $d_x=\infty$)

In the experiments the beam radius r, the power of the defocused beam and the transversal distances d_y between the welding and the defocused beam were varied. Due to the cooling of the welded plates to ambient temperature before the heating process was started, the longitudinal distances d_x between the welding and the defocused beam were not investigated in these experiments. After the completion of the experiments, the residual stresses were measured by X-ray diffraction method. In Table 1 some experimental results with different parameter sets regarding the stress reduction in the weld are listed. These stress reductions relate to the stresses in the reference weld.

Table 1. Longitudinal stresses in the weld centre (travel speed of the defocused beam of 5 mm/s)

Radius of the defocused beam *(mm)*	Power of the defocused beam / generated temperature by the defocused beam *(kW / °C)*	Transversal distance of beam centre from the weld centre *(mm)*	Longitudinal stresses in the weld on the top side (*MPa*)	Stress reduction on the top side *(%)*	Longitudinal stresses in the weld on the bottom side (*MPa*)	Stress reduction on the bottom side *(%)*
Reference	-	-	504.9 ±49.7	-	482.0 ±45.3	-
9.5	2.3 / 683	25	398.6 ±27.0	21	339.2 ±18.5	30
12.0	3.5 / 692	25	390.4 ±75.9	23	202.0 ±19.0	58
15.5	2 / 462	25	433.5 ±30.1	14	439.9 ±25.5	9
15.5	4 / 681	25	441.8 ±49.2	12	209.5 ±36.5	57
15.5	4 / 672	30	391.7 ±26.7	22	128.3 ±39.6	73
15.5	5 / 763	25	563.2 ±34.7	-12	18.2 ±22.2	96

4. Experimental results and discussion

As concluded from the simulation results the stress reduction in the weld takes places due to the generation of additional tensile stress regions in consequence of heating the material with the defocused beam up to several hundred degrees Celsius on both sides of the weld. This heat treatment generates compressive stresses which cause plastic deformations. During cooling these stresses switch to tensile stresses due to the material shrinkage, which unloads the weld by compressing the material region between the heat treated region and the weld. In other words, the stress reduction is based on a mechanical unloading effect of the weld due to these additional tensile stress zones.

In the experiments with the 5 kW fibre laser source, the weld cooled down to ambient temperature and contained high longitudinal stresses before the heat treatment with the defocused beam was executed. For this heating process, the material in a certain transversal distance to the weld has to be heated up to temperatures $T_{post,max}$ slightly above the stress relief annealing temperature for ferritic steels of about 700 °C. For lower temperatures, the experimental results listed in Table 1 show lower stress reductions. In the experiments with a defocused laser beam radius of 15.5 mm and a transversal distance of the beam to the weld of 25 mm, the stress reduction with 4 kW beam power is much higher on the bottom surface compared to the experiment with 2 kW. The reason is the lower generated temperature $T_{post,max}$ on the top surface (shown in Figure 5 for three different beam powers and two different transversal distances) of about 460 °C for 2 kW beam power compared to higher powers like 4 kW. This lower temperature on the top surfaces results in lower generated temperatures on the bottom surface and less plastic deformations on the bottom surface. Accordingly, during cooling to ambient temperature less tensile stresses are generated which results in less unloading of the weld. For higher temperatures the results in Table 1 show an even better stress reduction on the bottom surface with 5 kW beam power compared to 4 kW, because the generated temperatures at the bottom surface are higher. But on the top surface the temperatures ranging above 700 °C (cf. Figure 5) show no stress reduction but a small stress increase which is in the region of the measurement variation.

In addition to $T_{post,max}$, the assumed correlation of the geometric process parameters r and d_y for the defocused beam with the longitudinal weld stresses obtained from the simulation results in Figure 3 was verified by the experimental results, too. For the three different radii r given in Table 1 it was proven that the specific transversal distances d_y is most suitable to reduce the residual stresses in the weld increases with the radius of the defocused beam. According to the simulation results, the best stress mitigating effect of the process is assumed to be achieved for transversal distance of around the radius plus 12 mm by using a travel speed of the defocused beam of 15 mm/s. With lower speeds this distance is marginally increased as seen in Figure 4. The experimental results given in Table 1 for a travel speed of the defocused beam of 5 mm/s provide the most suitable transversal distance of the defocused beam to the weld at values of about the radius plus 13 mm - 15 mm, which confirms the simulation results (cf. Figure 3 with an increase of d_y of 3 mm by reducing the travel speed from 15 mm/s to 5 mm/s for a radius of 15 mm).

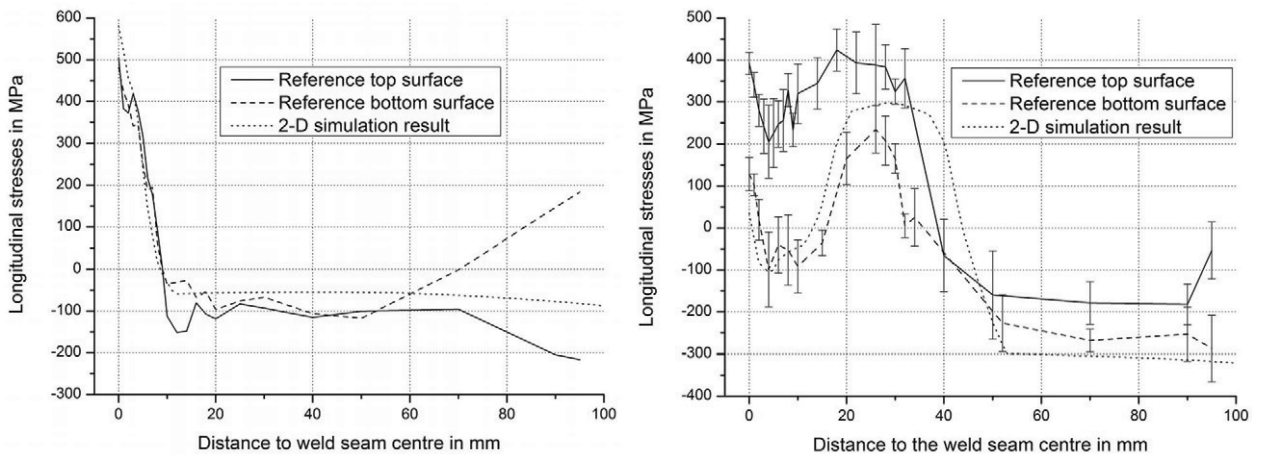

Figure 6. Comparison between experimental results of longitudinal stresses in a welded specimen (left, welding speed v_w=25 mm/s, welding power P_w=5 kW) and a heat treated welded specimen with 2D-simulation results (right, travel speed of the defocused beam v_{hf}=5 mm/s, heating power P_{hf}=4 kW, radius of the defocused beam r=15.5 mm, transversal distance from defocused beam to the weld d_y=30 mm, longitudinal interval d_x=∞)

The results of the parameter investigation by FEM-simulation were verified by the experimental results. In Figure 6 the experimentally measured longitudinal stresses of a reference weld (left) and of a post weld heat treated plate are compared with the corresponding simulation results. This comparison shows that the stress levels are not predictable with the used 2D-model for the parameter study.

Due to the duration of about 5 ms - 10 ms needed for beam deflection from one to the other side of the weld and of 60 ms for heating the material at one side before beam deflection to the other side, the weld region is heated by around 8 % - 17 % of the beam power. In the optimized FEM-model this effect arising from the deflection conditions is considered by implementing a second traveling heat source into the weld region with the mentioned partial power of the laser beam. The model of this heat source in the weld region comprises a cyclic area with a specified radius and a homogenously distributed power density analogously to the model for the heating field. With this simple optimization the two-dimensional simulation results plotted in the diagram shown in Figure 7 give a good accordance with the real longitudinal stresses measured in the experiment at the top surface of the workpiece.

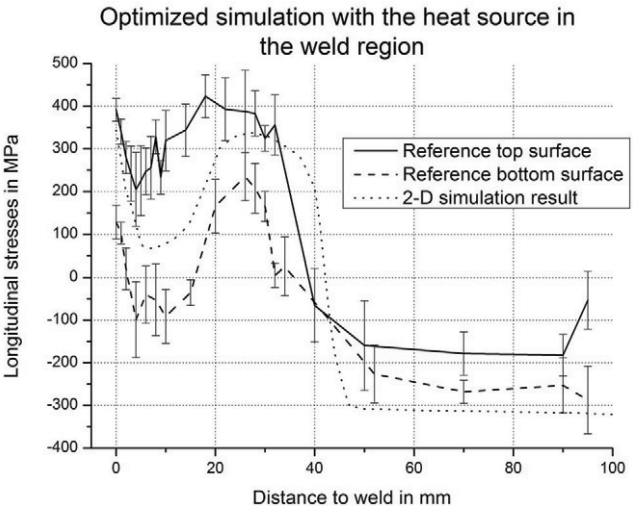

Figure 7. Comparison between experimental results of longitudinal stresses in a heat treated welded specimen with the optimized 2D-simulation results (welding speed v_w=25 mm/s, welding power P_w=5 kW, travel speed of the defocused beam v_{hf}=5 mm/s, heating power P_{hf}=4 kW, radius of the defocused beam r=15.5 mm, transversal distance from defocused beam to the weld d_y=30 mm, longitudinal interval d_x=∞)

As shown by the experimental results in Table 1 and Figure 6, the stress reduction at the bottom surface of the weld is much higher than at the top surface. The reason is the relation between the restored energy in the areas of elastic deformations on the top surface and the restored energy on the bottom surface. The weld on the top surface has nearly twice the width compared to the bottom surface. This is to say that the restored elastic energy on the top surface is higher than the restored elastic energy on the bottom surface. Thus, the mechanical effect of additional tensile stress regions on both sides of the weld is much higher on the bottom surface.

5. Conclusion

A new method of reducing high longitudinal residual stresses in laser beam welds has been suggested. The stress reduction occurs due to a mechanical unloading effect by the generation of additional tensile stress zones on both sides of the weld through heating up the material regions with a defocused laser beam to several hundred degrees Celsius. The tendencies shown by the simulation results were verified in experiments. The best results in the finite element simulation and in the experimental investigations were obtained with generated temperatures $T_{post,max}$ of about 700 °C. Lower temperatures cause less plastic deformations due to less stress relaxation that generate tensile stresses during cooling to ambient temperature. The experimental results for higher temperatures show that the depth effect can be increased, but in this case no stress reduction was measured on the top surface.

With this process it is possible to decrease the stresses in small welds with high stress gradients without any contact surfaces or additional equipment. Dependent on the component geometry and on the laser power it is possible to use different geometric parameters for this process. As a result, the most suitable transversal distance of the defocused beam to the weld d_y correlates with the radius of the defocused beam r. The travel speed during heating influences this correlation to a minor degree. According to the simulation and the experimental results, the most suitable transversal distance could be assumed for values of the radius plus 12±3 mm.

The FEM-simulation with the adiabatic 2D-model offered a qualified tool to define most suitable process parameter regions for the experimental investigations. The best experimental result shows a stress reduction of about 22 % on the top surface and of 73 % on the bottom surface of the 5 mm thick S355J2+N.

Acknowledgements

The authors would like to thank the Federation of Industrial Research Associations (AiF Arbeitsgemeinschaft industrieller Forschungsvereinigungen) and the German Federal Ministry for Trade, Industry and Technology (BMWi Bundesministerium für Wirtschaft und Technologie), for making this research possible by funding it in the Project 16139 N “Anwendung der Mehrstrahltechnik zur Reduzierung der Eigenspannungen bei EB- und LB-geschweißten Bauteilen“ (“Application of the multiple-beam-technique for residual stress reduction in EB and LB welded components”). In addition the authors would like to thank the HIGHYAG Lasertechnologie GmbH for providing their laser welding system for this research.

References

[1] Nitschke-Pagel, T.; Dilger, K.: Eigenspannungen in Schweißverbindungen - Teil 1: Ursachen der Eigenspannungsentstehung beim Schweißen. In: Schweißen und Schneiden, 58 (2006), 466-479
[2] Nitschke-Pagel, T.; Dilger, K.: Eigenspannungen in Schweißverbindungen - Teil 2: Bewertung von Eigenspannungen. In: Schweißen und Schneiden, 59 (2007), 23-32
[3] Han, S.; Lee, T.; Shin, B.: Residual stress relaxation of welded steel components under cyclic load. In: Steel research, 73 (2002), 414-420
[4] Brauss, M. E.; Pineault, J. A.; Eckersley, J. S.: Residual stress characterization of welds and post-weld processes using X-ray diffraction techniques. In: Process Control and Sensors for Manufacturing (Proceedings of the SPIE - The International Society for Optical Engineering), 3399 (1998), 196-204
[5] Sun, Z.: Residual stress in laser welded dissimilar steel tube-to-tube joints. In: Scripta metallurgica et materialia, 29 (1993), 633-637
[6] Mochizuki, M.: Control of welding residual stress for ensuring integrity against fatigue and stress–corrosion cracking. In: Nuclear Engineering and Design, 237 (2007), 107–123
[7[Nitschke-Pagel, T.; Dilger, K.: Eigenspannungen in Schweißverbindungen - Teil 3: Verringerung von Eigenspannungen. In: Schweißen und Schneiden, 59 (2007), 387-395
[8] Gabzdyl, J.; Johnson, A.; Williams, S.; Price, D.: Laser weld distortion control by cryogenic cooling. In: High-power Laser macroprocessing (Proceedings of the SPIE - The International Society for Optical Engineering), 4831 (2003), 269-274
[9] Guan, Q.; Zhang, C. X.; Guo, D. L.: Dynamic control of welding distortion by moving spot heat sink. In: Welding in the World, 33 (1994), 308-312
[10] Li, J.; Guan, Q.; Shi, Y. W.; Guo, D. L.: Stress and distortion mitigation technique for welding titanium alloy thin sheet. In: Science and technology of welding and joining, 9 (2004), 451-458
[11] Luan, G.; Li, G.; Li, C.; Dong C.: DC-LSND friction stir welding. In: 7th International Friction Stir Welding Symposium, Osaka, 2008

[12] Guan, Q.; Guo, D. L.; Li, C. Q.; Leggatt, R. H.: Low Stress Non-Distortion Welding (LSND) – A new Technique for Thin Materials. In: Welding in the World, 33 (1994) , 160-167
[13] Guan, Q.; Guo, D. L.; Zhang, C. X.; Li, J.: Low stress no distortion welding based on thermal tensioning effects for thin materials. In: The Paton Welding Journal, 12 (2006), 2-11
[14] van der Aa, E. M.; Hermans, M. J. M.; Richardson, I. M.: Control of Welding Residual Stress and Distortion by Addition of a Trailing Heat Sink, Mathematical Modelling of Weld Phenomena 8, Verlag der Technischen Universität Graz, 2007, 1053-1072
[15] ESI Group: Sysweld 2006 – Werkstoffkennwertdatenbank, 2006
[16] Gebhardt, M. O.; Quiroz, V.; Gumenyuk, A.; Rethmeier, M.: Restraint effects on stresses and strains in single-run high power laser beam welding of thick plates. Mathematical Modelling of Weld Phenomena 9, Verlag der Technischen Universität Graz, 2010, 1011-1033